

II. MICROWAVE SPECTROSCOPY*

Prof. M. W. P. Strandberg
Prof. R. L. Kyhl
Dr. B. D. Nageswara Rao
J. M. Andrews, Jr.
R. Huibonhoa

J. G. Ingersoll
P. F. Kellen
J. D. Kierstead
S. H. Lerman

J. W. Mayo
H. Pauwels
W. J. Schwabe
A. Fukumoto
J. Shah

A. AN APPLICATION OF MICROWAVE FREQUENCY ULTRASONICS TO THE MEASUREMENT OF THE FERMI SURFACE OF GALLIUM

This report is a summary of a Ph.D. thesis submitted to the Department of Physics, M.I.T., August 19, 1963.

What is believed to be the first application of microwave ultrasonics to the observation of magnetoacoustic oscillations in metals is described in the author's thesis. Difficulties in making single-crystal metal samples suitably thin and flat for this purpose and in bonding them to ultrasonic transducers have been overcome, to make what had hitherto been considered an impractical use of microwave ultrasonics into a very powerful one. The large values of $q\ell$ and $\omega\tau$ easily achieved at such frequencies provide the principal advantage over radio-frequency techniques.

The theory of ultrasonic attenuation in metals has been reviewed and a general expression for the electronic contribution to the attenuation in a metal with an arbitrary Fermi surface at an arbitrary frequency (but below the plasma frequency) derived. For the free-electron gas this expression reduces to the familiar results of Pippard.

The results of experiments on gallium for 6 different combinations of magnetic field and ultrasonic propagation directions are reported. Sixty-one series of magnetoacoustic oscillations are presented, of which 55 are tentatively identified as geometric resonances, and 6 as ultrasonic cyclotron resonances. These results suggest that the Fermi surface of gallium consists of many separate pieces, some of which are quite small and some of which give rise to rather high electron (or hole) effective mass. Many of the pieces seem to be less irregularly shaped than is suggested by the orthogonalized plane-wave model.

The velocity of propagation of longitudinal ultrasonic waves along the a, b, and c crystallographic directions of gallium is reported.

A peculiar phenomenon, suggestive of an additional mode of ultrasonic propagation in metals at microwave frequencies, was observed and a brief discussion is given in the thesis.

N. Tepley

*This work was supported in part by Purchase Order DDL BB-107 with Lincoln Laboratory, a center for research operated by Massachusetts Institute of Technology with the joint support of the U. S. Army, Navy, and Air Force under Air Force Contract AF19(604)-7400.

(II. MICROWAVE SPECTROSCOPY)

B. ULTRASONIC ATTENUATION IN SUPERCONDUCTORS

The scope of the measurements of the attenuation of L-band phonons in thin samples of superconducting and normal indium, reported previously,¹ has been extended to include both the temperature dependence and the magnetic-field orientation dependence. The experiments were carried out in a standard helium-four cryostat throughout a temperature range extending from slightly above 3.40°K (the critical temperature of indium) down to 1.22°K. The L-band ultrasonic rack and the low-temperature station employed in these measurements are shown in Fig. II-1.

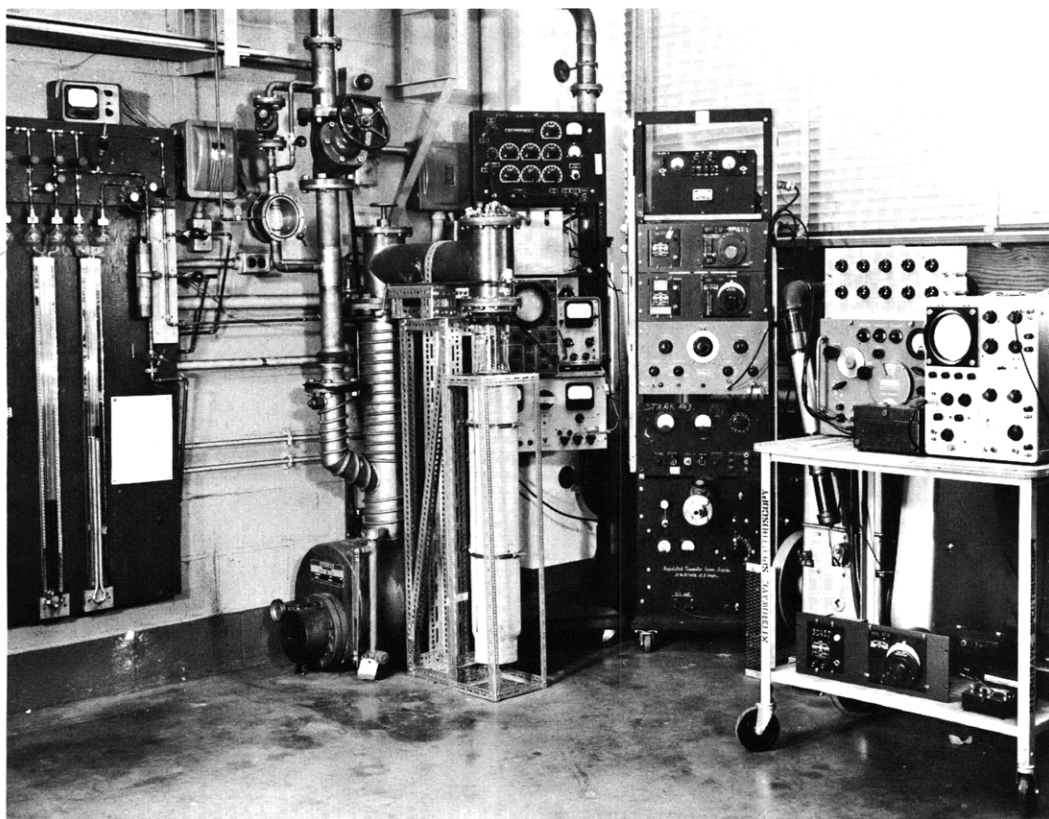


Fig. II-1. L-band ultrasonic rack and the low-temperature station.

The cryostat has been provided with a facility for automatic temperature regulation.² A close-up of the temperature regulator is shown in Fig. II-2. The helium vapor is evacuated through a thin-walled rubber tube that is contained within a pressure chamber. The reference pressure in this chamber is controlled by a large ballast tank, the pressure of which may be adjusted to any desired value. The pressure difference

(II. MICROWAVE SPECTROSCOPY)

between the reference chamber and the pump line collapses the thin-walled rubber tube until the pumping rate is equal to the boiling rate of the helium at the desired reference pressure. During the course of the experiment, this automatic temperature regulator is employed to keep the pressure constant over the boiling helium within 0.1 mm Hg,

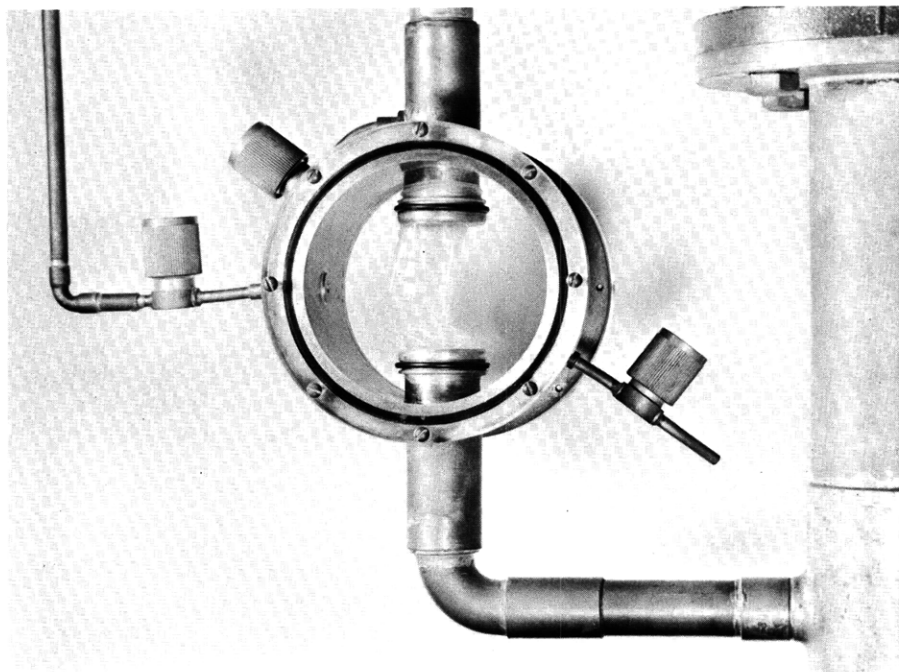


Fig. II-2. Automatic temperature regulator.

from 3.4°K to 1.7°K. Under equilibrium conditions, this corresponds to a maximum temperature fluctuation of 2×10^{-3} °K at the lower limit of its range. Below 1.7°K there is not sufficient gas pressure to collapse the rubber tube, and the temperature of the system must be regulated by manual adjustment of the pumping rate.

The magnetic field is supplied by superconducting Helmholtz coils. Each coil consists of 800 turns of niobium wire wound upon a brass coil form so that the mean diameter of the coils is 3 inches. The coil form is provided with clamps for mounting the L-band re-entrant cavities in either of two orientations — $\vec{H} \parallel \vec{q}$ or $\vec{H} \perp \vec{q}$, where q is the ultrasonic wave vector. The photograph in Fig. II-3 is a view of the superconducting magnet, and the sketch is a scale drawing defining the orientation of the H and q vectors with respect to the indium sample. The magnetic field may be determined within 0.2 per cent by measuring the current to the superconducting magnet with a precision ammeter.

The entire L-band ultrasonic cryostat head is shown assembled in Fig. II-4. An

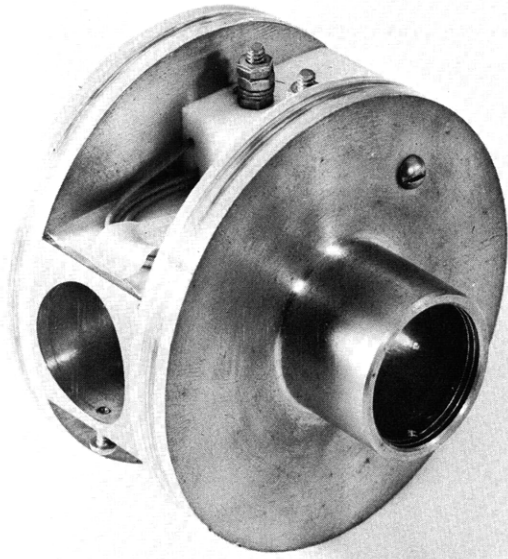


Fig. II-3.

Upper: photograph of the superconducting Helmholtz coils.
 Lower: sketch illustrating the orientation of the H and q vectors with respect to the indium sample. (The transducer-sample system has a circular cross section.)

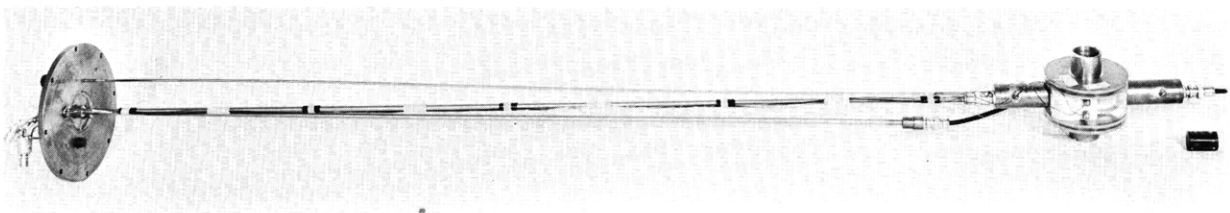
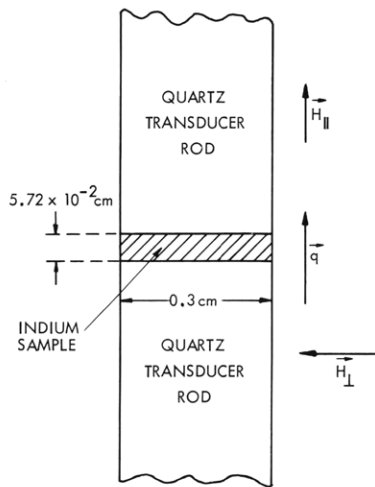


Fig. II-4. Assembled L-band ultrasonic cryostat head.

(II. MICROWAVE SPECTROSCOPY)

exploded view of the L-band re-entrant cavities and a description of the electronic apparatus used for the generation and detection of the ultrasonic pulses has been included in a previous report.¹

1. Energy Gap

The theory of superconductivity proposed by Bardeen, Cooper, and Schrieffer³ (BCS) includes a calculation of the ratio of the electronic contribution to the ultrasonic attenuation coefficient of a metal in the superconducting state to that of the metal in the normal state.

$$\frac{a_s}{a_n} = 2f(\epsilon), \quad (1)$$

where $f(\epsilon)$ is the Fermi function

$$f(\epsilon) = \frac{1}{e^{\epsilon(T)/kT} + 1} \quad (2)$$

and $\epsilon(T)$ is the temperature-dependent superconducting energy gap. A graph of the normalized energy gap $\epsilon(T)/\epsilon(0)$ is shown in Fig. II-5a as a function of reduced temperature. The normalized superconducting attenuation coefficient of Eq. 1 is represented

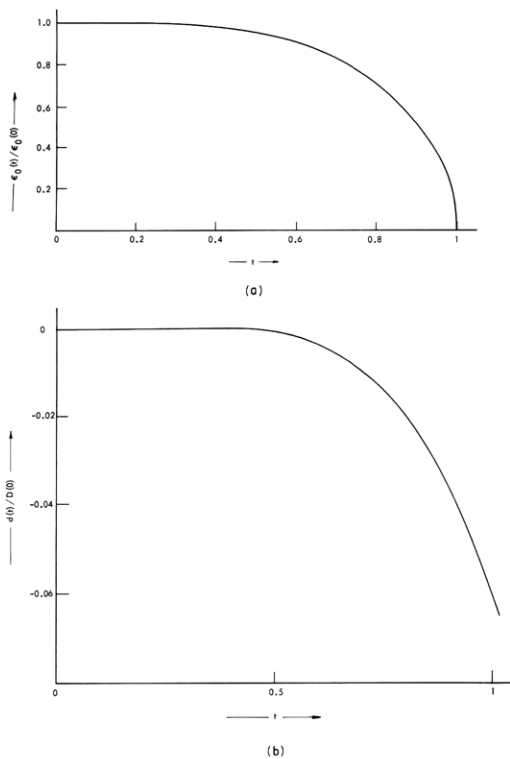


Fig. II-5. (a) Temperature dependence of the superconducting energy gap (after Bardeen, Cooper, and Schrieffer³).
(b) Experimental temperature dependence of $d(t)/D(0)$ in polycrystalline indium at 28.5 mc (from the work of Morse⁵).

(II. MICROWAVE SPECTROSCOPY)

by the solid line in Fig. II-7a as a function of the reduced temperature T/T_c . The essence of the BCS theory is that in certain metals that are cooled below some critical temperature T_c that is characteristic of the metal, it is energetically favorable for the conduction electrons in the immediate vicinity of the Fermi surface to condense into quasi particles, each containing a pair of electrons whose spin and momentum vectors are equal and opposite. Since the quasi particles possess zero total momentum, they do not contribute to phonon scattering. The sharp decrease of Eq. 1 directly below $t=1$ reflects the decreasing fraction of normal electrons.

The experimental procedure is to pump on the liquid helium until some desired temperature is reached, and then to close the valve connecting the automatic regulator ballast tank to the cryostat. The automatic regulator will then hold this temperature within 2×10^{-3} °K for any desired length of time until the helium has evaporated. The transmitter produces periodic pulses of rf power which are converted into acoustic pulses by one re-entrant cavity, are passed down the first quartz transducer rod, through the sample, and through the second quartz transducer rod, and are reconverted into rf energy in the second re-entrant cavity. After detection, this transmitted pulse is

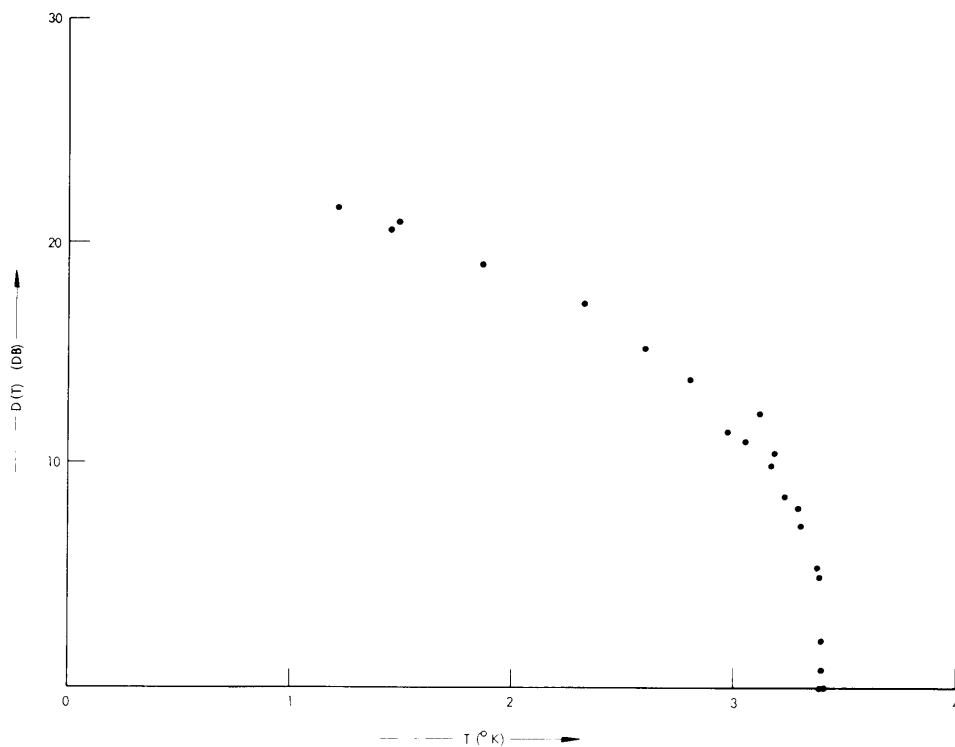


Fig. II-6. Experimental values of the difference $D(t)$ in the electronic contribution to the ultrasonic attenuation coefficient between the superconducting and the normal states for indium, 5.72×10^{-2} cm thick at 0.91 kmc.

(II. MICROWAVE SPECTROSCOPY)

displayed on an oscilloscope beside an rf calibration pulse, which has been injected into the system in order to eliminate the need for measuring the nonlinear character of the detection process. While the sample is in the superconducting state, the height of the calibration pulse is adjusted to equal the signal pulse. The sample is then returned to the normal state by switching on a current to the superconducting magnet which is sufficient to produce a magnetic field greater than the critical field of the indium at that temperature. The height of the calibration pulse is then reduced to equal the height of the signal pulse by use of a calibrated attenuator. Therefore, the quantity that is recorded is $D(T)$, a measure, in decibels, of the difference in the transmitted pulse height when the metal sample is switched between the superconducting and the normal states. The experimental values of $D(T)$ obtained for a disc of indium 5.72×10^{-2} cm thick at 0.91 kmc are displayed in Fig. II-6.

In order to relate $D(T)$ to Eq. 1 it is necessary to extrapolate the measurements to $T=0^\circ\text{K}$, and to obtain the temperature dependence of the normal attenuation coefficient.

$$\frac{a_s(T)}{a_n(T)} = 1 - \frac{D(T)}{D(0)} \cdot \frac{a_n(0)}{a_n(T)} \quad (3)$$

The short-term stability of the apparatus was sufficient to determine $D(T)$ within a few per cent by averaging approximately 10 measurements. The mean-square deviation was usually around 0.3 db but sometimes rose as high as 0.5 db. It was not possible, however, to determine $a_n(0)/a_n(T)$ accurately in these experiments. The strong temperature dependence of the dielectric constant of liquid helium above the λ -point requires continual adjustment of the apparatus as the temperature is lowered. This and other factors contribute to a long-term instability of the apparatus.

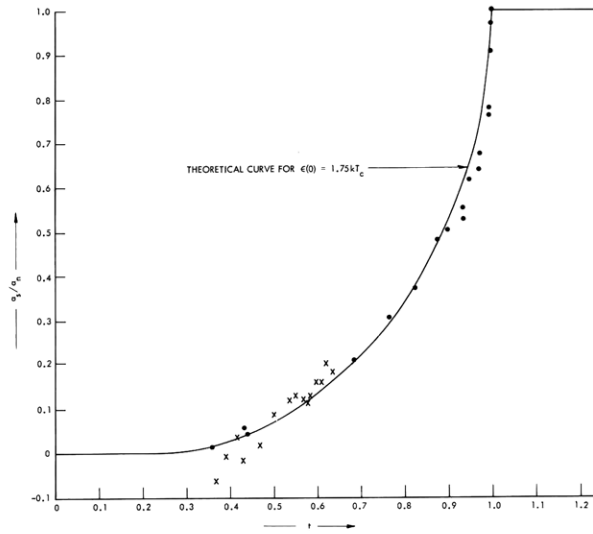
The temperature dependence of the normal attenuation coefficient $a_n(T)$ is caused by the variation of the mean-free path of the conduction electrons as a function of temperature. From the initial work of Bömmel⁴ on lead it can be seen that, at 27 mc, $a_n(T)$ rises rapidly as the temperature is lowered from 10°K to 4°K . Below 4°K it approaches a constant value determined by impurity, grain boundary, and geometric boundary scattering. Since it is the ratio of the electronic mean-free path to the ultrasonic wavelength that is important in ultrasonic attenuation, it is evident that at higher frequencies this transition should begin at a higher temperature.

The complicated dependence of $a_n(T)$ upon sample and frequency makes it difficult to ascertain the effect of this quantity upon our interpretation of the $D(T)$ measurements, but it is possible to obtain an estimate of the upper limit. To this end, we define a quantity $d(T)$ for the metal in the normal state which represents the deviation in decibels of the transmitted pulse height at any temperature T from that at absolute zero. This quantity is related to $a_n(T)/a_n(0)$ by the following equation.

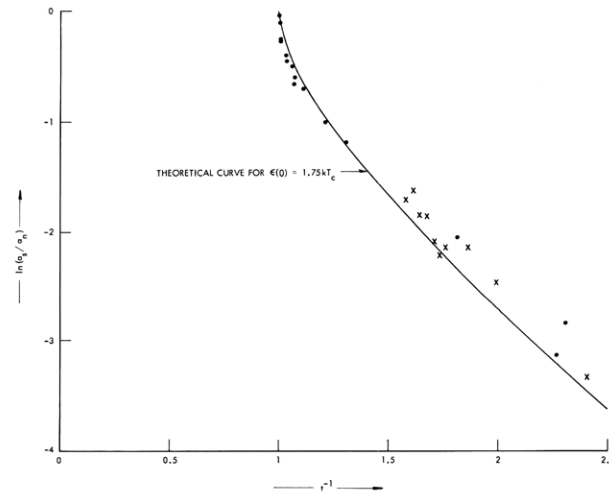
(II. MICROWAVE SPECTROSCOPY)

$$\frac{d(T)}{D(0)} = 1 - \frac{a_n(T)}{a_n(0)} \quad (4)$$

and Eq. 3 becomes



(a)



(b)

Fig. II-7. (a) Normalized superconducting attenuation coefficient. Experimental temperature-dependent data have been superimposed according to Eq. 5, with $d(t) = 0$, upon a plot of Eq. 1, with $\epsilon(0) = 1.75 kT_c$.
 (b) Logarithm of the data of (a) as a function of inverse reduced temperature. The asymptotic value of the curve serves to fix the absolute value of the superconducting energy gap at absolute zero.

(II. MICROWAVE SPECTROSCOPY)

$$\frac{a_s(t)}{a_n(t)} = 1 - \frac{D(t)}{D(0)-d(t)}. \quad (5)$$

Here, as a matter of convenience, we have expressed the functional relationships in terms of the reduced temperature $t \equiv T/T_c$. The temperature dependence of $d(t)/D(0)$ has been extracted from the data of Morse⁵ on polycrystalline indium at 28.5 mc. It is plotted in Fig. II-5b. The magnitude of $d(t)$, as well as the position of the knee at which $d(t)$ becomes constant, is likely to be different for our experiment. The most rapid variation of $d(t)$ occurs near $t=1$, and it has been possible to establish from our measurements

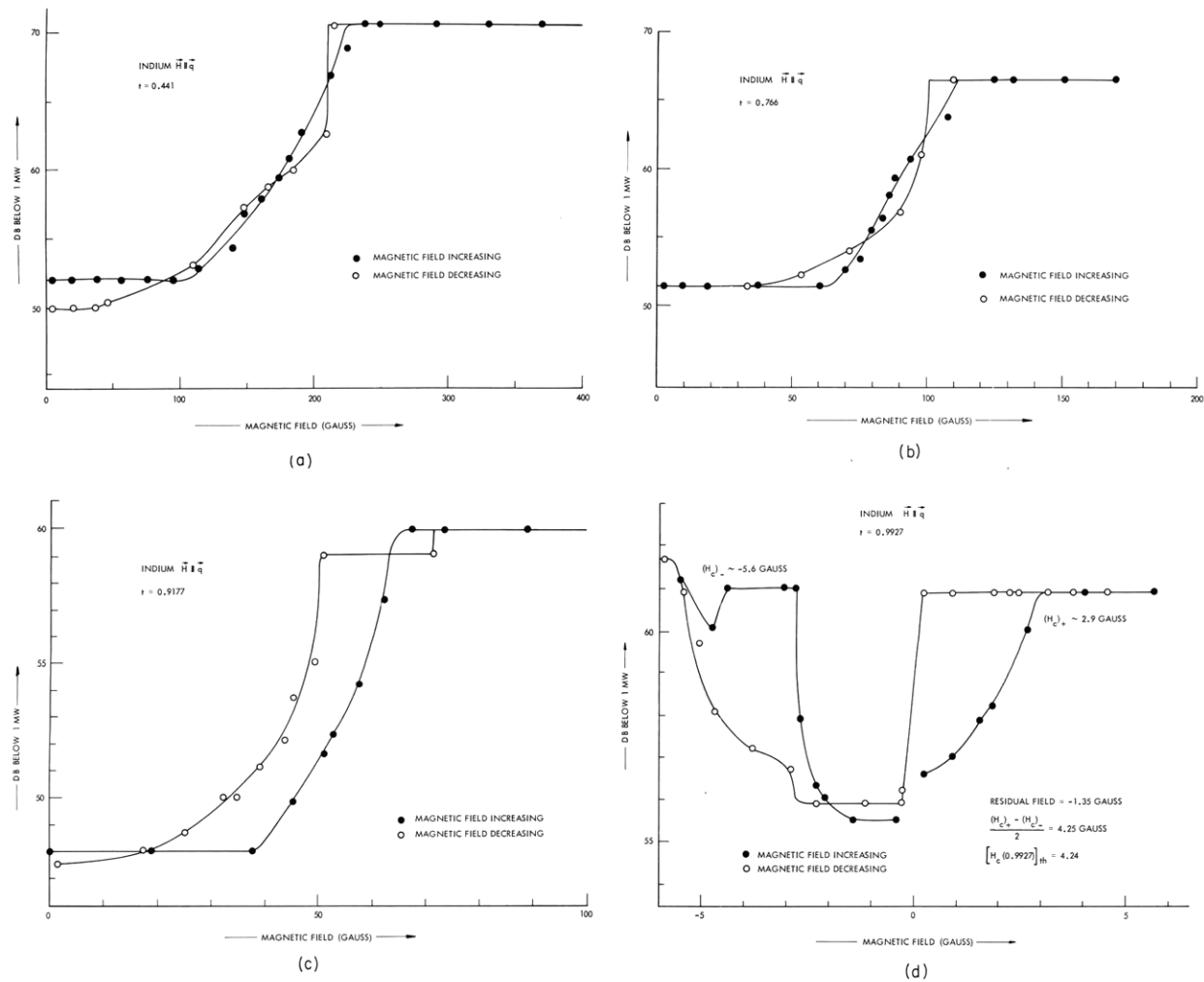


Fig. II-8. Attenuation of L-band ultrasonic pulses in indium as a function of external magnetic field. (a) $t = 0.441$; (b) $t = 0.766$; (c) $t = 0.9177$; (d) $t = 0.9927$.

(II. MICROWAVE SPECTROSCOPY)

that $|d(t)| \leq 3$ db at $t=1$. This means that $d(t)/D(0)$ for our experiment is probably not larger than 2 or 3 times that shown for Morse's data in Fig. II-5b, a fact that could affect our measurements a_s/a_n by 10 or 20 per cent, at most, within a small region of temperature above $t=0.9$. Below this temperature, the effect diminishes rapidly to a negligible value at $t=0.6$.

In the light of these considerations, we shall delete $d(t)$ from Eq. 5 and superpose the data expressed in Fig. II-6 upon a theoretical curve obtained from Eq. 1. This function has been evaluated for the superconducting energy gap $\epsilon(0)=1.75kT_c$ predicted for all superconductors in the BCS approximation.³ The comparison of our data with the BCS theory is shown in Fig. II-7a. The extrapolated value $D(0)$ was obtained by fitting all of the experimental points $D(t)$ to Eq. 1 for temperatures less than $t=0.9$. Points at higher temperatures did not fit well. A possible cause may be the exclusion of the unknown $d(t)$ function. At low temperatures $D(t)$ approaches 21 db, and it becomes increasingly difficult to make accurate measurements. Consequently, another run was made with the effort concentrated in a region $0.35 < t < 0.65$. These additional points are shown by crosses in Fig. II-7a. Each of these points consists of an average of 9, or more, separate measurements of $D(t)$. The mean-square deviation was usually 0.3 db, but sometimes rose as high as 0.5 db. The scatter of the points at the lower temperatures reflects the increased difficulty of making measurements as $D(t)$ approached its maximum value.

The measurements for $t < 0.6$ are especially important for a comparison with energy-gap theory, and a much more sensitive evaluation of the data can be obtained by plotting $\ln(a_s/a_n)$ as a function of t^{-1} . This is shown in Fig. II-7b, in which both the theoretical curve and the position of the experimental points depend upon the choice $\epsilon(0) = 1.75kT_c$. The asymptotic value of this curve serves to fix the absolute value of the superconducting energy gap $\epsilon(0)$. Scatter of the experimental points blurs the determination of $\epsilon(0)$ within a region that is $\approx \pm 10$ per cent. A choice of $\epsilon(0)$ outside of this region, however, does not lead to self-consistency.

2. Magnetic-Field Data

The magnetic-field dependence of the ultrasonic attenuation in the indium sample was measured at four temperatures between 1.50°K and 3.40°K with $\vec{H} \parallel \vec{q}$. These measurements are shown in Fig. II-8. As the magnetic field is increased, the onset of the intermediate state is denoted $H_e(t)$; the end of the intermediate state, that is, the beginning of the normal state, is denoted $H_c(t)$. If H is increased to a value somewhat larger than $H_c(t)$ and then reduced, the normal state persists for values of $H < H_c(t)$ until the magnetic field reaches some value $H_l(t)$. At this point the ultrasonic attenuation decreases suddenly, with an infinite slope, to some value that is characteristic of the intermediate state of the superconductor. This is an example of the "supercooling"

(II. MICROWAVE SPECTROSCOPY)

Table II-1. Summary of temperature-dependence of magnetic-field data.

t	Figure No.	Orientation	$H_e(t)$	$H_c(t)$	$H_l(t)$	$H_p(t)$	n^a	ϕ	Accuracy
.389	not shown	$\vec{H} \perp \vec{q}$	174	235.7	—	240	.26	—	good
.441	II-8a	$\vec{H} \parallel \vec{q}$	110	224	210	228	.51	.12	fair ^b
.621	not shown	$\vec{H} \perp \vec{q}$	126	167	—	174	.25	—	good
.766	II-8b	$\vec{H} \parallel \vec{q}$	65	111	100	117	.41	.19	fair ^b
.9177	II-8c	$\vec{H} \parallel \vec{q}$	38	64	51	45	.41	.36	fair ^b
.9927	II-8d	$\vec{H} \parallel \vec{q}$	1.4	4.25	1.75	4.24	.67	.83	fair ^b

^aAverage values: $\bar{n}_{\parallel} = 0.50$, $\bar{n}_{\perp} = 0.255$.

^bValues obtained by extrapolation of the curves of Fig. II-8.

effect in a superconductor — actually a misnomer, since the process is carried out at constant temperature. The name, of course, derives from the analogy to the supercooling of a gas below its liquefaction temperature. The sudden drop in the ultrasonic attenuation at $H_l(t)$ justifies to some extent the procedure of obtaining the experimental values for $H_l(t)$ by means of a vertical extrapolation. The quantities $H_e(t)$, $H_c(t)$, and $H_l(t)$ obtained from the graphs are shown in Table II-1 as functions of reduced temperature and magnetic-field orientation. These have been labeled "fair" in the accuracy column. Their interpretation should be viewed as qualitative only, and they do not represent the ultimate that can be achieved by using our experimental method.

In a later run, the magnetic-field orientation was changed so that $\vec{H} \perp \vec{q}$. No magnetic-field plots were made during this run; rather H_e and H_c were determined as accurately as possible by repeated observation. The main purpose of this measurement was to obtain a check on the calculated ratio of the field of the superconducting magnet to the applied current. The agreement was found to be well within 1 gauss, the approximate resolution of the measuring technique. These experimental values are labeled "good" in the accuracy column of Table II-1 and probably represent about the best accuracy that can be obtained from this particular experimental configuration.

An interesting demonstration of the sensitivity of the ultrasonic technique can be seen in the interpretation of the data in Fig. II-8, taken at $t=0.9927$. At this temperature deviations from the parabolic law are negligible, and the theoretical value of the critical field is 4.24 gauss. Observations of the attenuation were made for both

(II. MICROWAVE SPECTROSCOPY)

positive and negative values of the magnetic field, and the resulting plot is not symmetric about $H=0$. The asymmetry suggests a residual magnetic field of -1.35 gauss, which is probably caused by a combination of the earth's magnetic field and the small magnetization of the surrounding experimental apparatus. When this residual field is subtracted from the observed critical values, an experimental value $H_c(0.9927) = 4.25$ gauss results.

3. Phase Transition

A theory of the phase transition in superconductors has been worked out by Faber⁶ and is based upon a simplified model specifying the conditions under which a superconducting nucleus is able to grow in the normal metal. Faber's work has indicated that nucleation occurs at certain flaws in the metal which are not related to surface conditions, impurity content or crystal boundaries. It is convenient to define a quantity ϕ which is a measure of the degree of supercooling. Recalling that the magnetic energy is quadratic in H , we define a quantity H_ℓ that is the value of the magnetic field at the point at which nucleation occurs, and we have

$$\phi(t) = 1 - \frac{H_\ell^2(t)}{H_c^2(t)}. \quad (6)$$

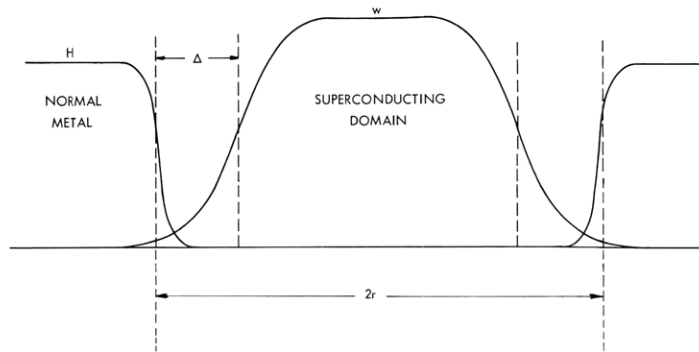


Fig. II-9. Interphase boundary Δ between a superconducting domain of radius r and the normal metal. (w denotes the superconducting order parameter and H is the external magnetic field. Actually, $\Delta \ll r$.)

The quantities $\phi(t)$ calculated from our data have been included in Table II-1.

Faber assumes that the flaws are domains in which the surface energy parameter Δ is negative. The quantity Δ may be identified as the width of the interphase boundary, and, according to a concept that is due to Pippard, this width is finite because the edge of the superconducting phase does not coincide with the edge of the normal phase. (See

(II. MICROWAVE SPECTROSCOPY)

Fig. II-9.) A further simplifying assumption of Faber is that $\Delta(r)$ is a negative constant for $r < a$, varies linearly from 0 to its maximum positive value for $a < r < b$, and is a positive constant for $r > b$. It is assumed that $b \gg a, \Delta$. From Fig. II-9 it is evident that $\Delta \approx \xi - \lambda$, where the coherence length ξ is the region in which the gradient of the Gorter-Casimir order parameter $w(t)$ is large, and λ is the magnetic-field penetration depth. Both vary as $(1 - t^4)^{-1/2}$, so that

$$\Delta(t) = \Delta(0) (1-t^4)^{-1/2}. \quad (7)$$

The analysis of Faber is carried out by writing down the Gibbs free energy of a section of the normal metal which contains a spheroidal volume of superconducting metal. By setting $dG/dr \leq 0$, a condition that allows the domain to grow is obtained.

$$\phi(t) = (1-n) \frac{2\Delta(t)}{r} \left[1 - \frac{\Delta(t)}{2r} + \dots \right] + n, \quad (8)$$

where n is the demagnetization coefficient, and r is the minor semiaxis of the spheroid. For our sample it turns out that Δ/r and n are both very small. Anticipating this

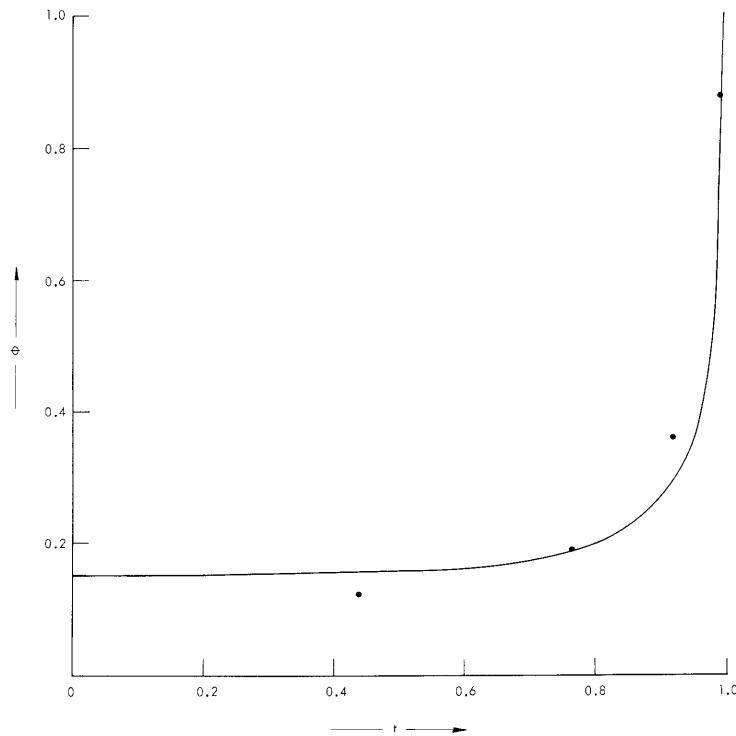


Fig. II-10. The degree of supercooling ϕ as a function of reduced temperature. Experimental values have been superimposed upon a plot of the theoretical prediction of Faber.⁶

(II. MICROWAVE SPECTROSCOPY)

result, we have

$$\phi(t) = \frac{2\Delta(0)}{r} (1-t^4)^{-1/2}. \quad (9)$$

Our data for $\phi(t)$ have been fitted to Eq. 9 by setting $2\Delta(0)/r = 0.15$, as shown in Fig. II-10. The best experimental value for the interphase surface-energy parameter for indium is $\Delta(0) = 3.40 \times 10^{-5}$ cm.⁸ These considerations lead to an estimate of the initial size and shape of the superconducting domains as our indium sample passes from the normal into the intermediate state: diameter, $2r = 9.0 \times 10^{-4}$ cm. The fact that $n \approx 0$ reveals that the intermediate state consists of long rods whose average direction is parallel to the magnetic field. These results are in close agreement with those of Faber whose work was based upon measurements of the Meissner effect in long bars of tin.

4. Critical Field

The temperature dependence of the critical field is given approximately by the

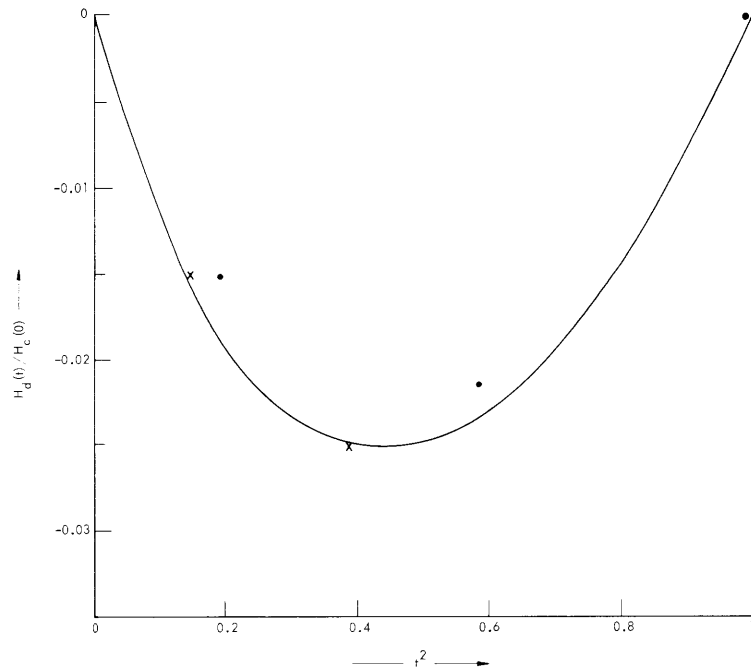


Fig. II-11. Experimental deviation of the critical field of indium from the parabolic law after Shaw, et al.¹⁰ Our $H_c(t)$ values from Table II-1 have been superimposed upon this curve. The points X were carefully determined from repeated observation. The points • were obtained from the curves of Fig. II-8 and are only approximate.

(II. MICROWAVE SPECTROSCOPY)

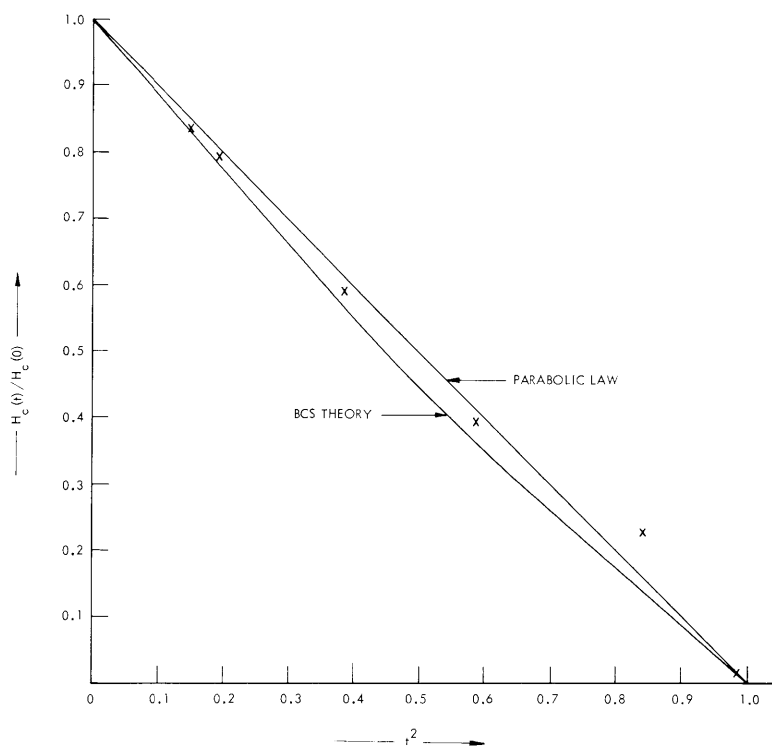


Fig. II-12. Temperature dependence of the critical field. Solid curves are the theoretical predictions according to Bardeen, Cooper, and Schrieffer,³ and Gorter-Casimir.⁹ Our experimental values have been superimposed.

parabolic law of the Gorter-Casimir two-fluid model.⁹

$$H_p(t) = H_c(0)(1-t^2) \tag{10}$$

The deviation of indium from this law has been measured by Shaw, Mapother, and Hopkins.¹⁰ The solid curve of Fig. II-11 shows their experimental results. The deviation $H_d(t)$ is defined by

$$H_d(t) = H_c(t) - H_p(t). \tag{11}$$

Our experimental values of $H_c(t)$ listed in Table II-1 are superimposed upon the solid curve of Fig. II-11. The points denoted x are the very carefully determined values from the $\vec{H} \perp \vec{q}$ run.

The BCS theory of superconductivity predicts a deviation of H_c from the parabolic law.³ The theoretical results are shown in Fig. II-12. Our experimental data have been superimposed upon this curve also. Although most of our results are reasonably consistent with the experimental work of others, it can be seen that the deviation from

(II. MICROWAVE SPECTROSCOPY)

the Gorter-Casimir theory is not as large as the BCS theory predicts. The single point indicating the large deviation at $t^2 = 0.84$ also shows up as a large deviation in Fig. II-7a at $t = 0.92$. This was the first point to be measured after the helium transfer, and it is likely that the cryostat had not reached thermal equilibrium. Thus the temperature determined from the vapor pressure of the helium may not have been equal to the temperature of the sample. Postulating a sample temperature of $t = 0.87$ brings both points into close agreement with the theoretical curves.

5. Demagnetization Coefficient

With the new superconducting magnet, it has been possible to study the orientation dependence of the demagnetization coefficient that is proportional to

$$n = 1 - \frac{H_e}{H_c}, \quad (12)$$

where $H_e(t)$ denotes the value of the magnetic field at the point at which the sample enters the intermediate state. The demagnetization coefficient $4\pi n$ is related to the orientation of the external magnetic field with respect to the geometry of the sample, but the more refined measurements of the $\vec{H} \perp \vec{q}$ run indicate that it is independent of temperature. Strictly speaking, the demagnetization coefficient is defined only for ellipsoids in which the magnetization is independent of position, and its application to our sample (Fig. II-3) is not rigorously justified. Nevertheless, it is interesting to compare our values with the theory. A theorem of the magnetization of macroscopic bodies states that the sum of the demagnetization coefficient around three mutually perpendicular axes is 4π . Thus

$$\sum_{i=1}^3 n_i = 1. \quad (13)$$

The average of the experimental values of n taken from Table II-1 yields

$$2\bar{n}_\perp + \bar{n}_\parallel = 1.01. \quad (14)$$

The agreement is somewhat fortuitous, in the light of the large deviations of the n_\parallel values in Table II-1. We can conclude, however, that the interpretation of the first knee $H_e(t)$ of the a vs. H curves of Fig. II-8 as the onset of the intermediate state is probably correct.

J. M. Andrews, Jr.

(II. MICROWAVE SPECTROSCOPY)

References

1. J. M. Andrews, Jr., Ultrasonic attenuation in superconductors, Quarterly Progress Report No. 70, Research Laboratory of Electronics, M.I.T., July 15, 1963, pp. 8-17.
2. E. J. Walker, Rev. Sci. Instr. 30, 834-835 (1959).
3. J. Bardeen, L. N. Cooper, and J. R. Schrieffer, Phys. Rev. 108, 1175 (1957).
4. H. E. Bömmel, Phys. Rev. 96, 220 (1954).
5. R. W. Morse, Progress in Cryogenics, Vol. 1, edited by K. Mendelssohn (Heywood and Company, Ltd., London, 1959), p. 221.
6. T. E. Faber, Proc. Roy. Soc. (London) 214, 392 (1952).
7. A. B. Pippard, Proc. Camb. Phil. Soc. 47, 617 (1951).
8. E. A. Lynton, Superconductivity (Methuen and Company, Ltd., London, 1962), p. 63.
9. C. J. Gorter and H. B. G. Casimir, Physik. Z. 35, 963 (1934); Z. Tech. Physik 15, 539 (1934); Physica 1, 305 (1934).
10. R. W. Shaw, D. E. Mapother, and D. C. Hopkins, Phys. Rev. 120, 88 (1960).

